A Genome-Wide Association Study Reveals a Novel Regulator of Ovule Number and Fertility in *Arabidopsis thaliana*

Jing Yuan[1,2] and Sharon A. Kessler[1,2*]

[1]Department of Botany and Plant Pathology, Purdue University, West Lafayette, IN 47907, USA

[2]Purdue Center for Plant Biology, Purdue University, West Lafayette, IN 47907, USA

***** Corresponding author
Email: sakessler@purdue.edu

Abstract

Ovules contain the female gametophytes which are fertilized during pollination to initiate seed development. Thus, the number of ovules that are produced during flower development is an important determinant of seed crop yield and plant fitness. Mutants with pleiotropic effects on development often alter the number of ovules, but specific regulators of ovule number have been difficult to identify in traditional mutant screens. We used natural variation in Arabidopsis accessions to identify new genes involved in the regulation of ovule number. The ovule numbers per flower of 189 Arabidopsis accessions were determined and found to have broad phenotypic variation that ranged from 39 ovules to 84 ovules per pistil. Genome-Wide Association tests revealed several genomic regions that are associated with ovule number. T-DNA insertion lines in candidate genes from the most significantly associated loci were screened for ovule number phenotypes. The *NEW ENHANCER of ROOT DWARFISM (NERD1)* gene was found to have pleiotropic effects on plant fertility that include regulation of ovule number

and both male and female gametophyte development. Overexpression of NERD1 increased ovule number per fruit in a background-dependent manner and more than doubled the total number of flowers produced in all backgrounds tested, indicating that manipulation of NERD1 levels can be used to increase plant productivity.

Key Words

Ovule number, NERD1, Arabidopsis, Branching, Carpel Margin Meristem, GWAS

Introduction

During plant reproduction, pollen tubes deliver two sperm cells to female gametophytes contained within ovules. This allows double fertilization to occur in order to produce the embryo and endosperm in the developing seed. Angiosperms with all kinds of pollination syndromes (insect-, wind-, and self-pollinated) produce much more pollen than ovules in order to ensure successful pollination. For example, most soybean varieties produce only 2 ovules per flower, but more than 3,000 pollen grains, a 1,500-fold difference[1]. Wind-pollinated plants such as maize have an even more extreme difference in pollen production vs. ovule production per plant, with more than 1 million pollen grains versus an average of 250 ovules per plant (a 4000-fold difference[2]). *Arabidopsis thaliana*, which is a self-pollinating plant, also produces an excess of pollen, with at least 2000 pollen grains per flower compared to an average of 60 ovules per flower[3]. Since pollen is produced in excess, in self-pollinated plants the number of ovules (i.e. female gametes) sets the maximum seed number per flower.

The ability to manipulate ovule number to increase the reproductive potential of plants requires an understanding of the molecular pathways that control ovule initiation.
The model plant *Arabidopsis thaliana* produces flowers with four whorls of organs: sepals, petals, stamens, and carpels. The inner whorls (3 and 4) are responsible for sexual reproduction, with pollen (the male gametophytes) produced in the whorl 3 stamens and the female gametophytes (also known as the embryo sacs), produced in ovules contained within the whorl 4 carpels. Specification of the 4 whorls is controlled by the "ABC" genes, with the C-class gene AGAMOUS (AG) a major regulator of carpel development[4].

In Arabidopsis, ovules are initiated from the carpel margin meristem (CMM) at stage 9 of floral development[5]. The Arabidopsis gynoecium comprises two carpels that are fused vertically at their margins [6]. The CMM develops on the adaxial face of the carpels (inside the fused carpel cylinder) and will give rise to the placenta, ovules, septum, transmitting tract, style, and stigma. Once the placenta is specified, all of the ovule primordia are initiated at the same time[7]. Subsequently, each primordium will be patterned into three different regions: the funiculus, which connects the ovule to the septum; the chalaza, which gives rise to the integuments; and the nucellus, which gives rise to the embryo sac. Ovule development concludes with the specification of the megaspore mother cell within the nucellus which undergoes meiosis followed by three rounds of mitosis to form the mature haploid embryo sac (reviewed in[8]).

In Arabidopsis, CMM development requires coordination of transcriptional regulators

involved in meristem function with hormone signaling (reviewed in[6]). Most mutants that have been reported to affect ovule number have pleiotropic effects related to the establishment of polarity and boundaries during gynoecial development (reviewed in [9]). For example, the *AINTEGUMENTA* (*ANT*) transcription factor regulates organ initiation and cell divisions during flower development[10]. *ANT* acts redundantly with the related gene *AINTEGUMENTA-LIKE6/PLETHORA3* to regulate carpel margin development and fusion which leads to a modest reduction in ovule number. This phenotype is exacerbated when *ant* is combined with mutations in other carpel development transcriptional regulators, such as *SEUSS* (*SEU*), *LEUNIG* (*LUG*), *SHATTERPROOF1* and *2* (*SHP1* and *SHP2*), *CRABSCLAW* (*CRC*), *FILAMENTOUS FLOWER* (*FIL*), and *YABBY3* (*YAB3*). Mutant combinations between *ant* and these mutants leads to severe defects in carpel fusion coupled with severe reductions in the marginal tissues that give rise to the CMM (summarized in[6]). An extreme example is the double mutant *seu-3 ant-1* which results in a complete loss of ovule initiation due to defects in CMM development[11]. The organ boundary genes, *CUP-SHAPED COTYLEDON1* and *2* (*CUC1* and *CUC2*), are also required for CMM development and subsequent ovule initiation. *ant cuc2* mutants with *cuc1* levels decreased specifically in the CMM by an RNAi construct driven by the *SEEDSTICK* promoter show an 80% reduction in ovule number, indicating that *ANT* controls cell proliferation while *CUC1/2* are necessary to set up the boundaries that allow ovule primordia to be initiated[12].

Plant hormones are also involved in gynoecium development and can have both indirect and direct effects on ovule number. Auxin biosynthesis, transport, signaling, and transport mutants have varying effects on gynoecium development and patterning,

many of which lead to pleiotropic effects on tissues and organs derived from the CMM[13]. Treatment of developing flowers with the auxin polar transport inhibitor NPA showed that an apical-basal auxin gradient in the developing gynoecium is necessary for patterning events that lead to ovule initiation[13]. Cytokinin has also been implicated in ovule initiation and development in Arabidopsis. Notably, triple mutants in the *ARABIDOPSIS HISTIDINE KINASE* (*AHK*) cytokinin receptors, *AHK2*, *AHK3*, and *AHK4/CRE1*, displayed a 90% reduction in ovule number due to decreased cytokinin signaling[14]. Conversely, double mutants in the cytokinin degrading cytokinin oxidases/dehydrogenases (CKXs) displayed higher cytokinin levels in inflorescences and produced more than double the number of ovules as in wild-type controls[15]. Brassinosteroids (BR) may also be positive regulators of ovule initiation. Gain-of-function mutants in the BR-induced transcription factor *BZR1* had increased ovule number per flower while BR-deficient and insensitive mutants had decreased ovule number compared to wild-type controls. Upregulation of the ovule regulators *ANT* and *HULLENLOS* (*HUL*) was correlated with *BZR1* activity, indicating the BR signaling positively regulates ovule development[16].

To date, research on the factors controlling ovule number has been limited to the analyses of mutants that have been identified based on pleiotropic effects on gynoecium development. In an attempt to identify loci that regulate ovule number without affecting other aspects of flower development, we took advantage of natural variation in ovule number in Arabidopsis accessions from diverse geographical locations. Over 7,000 natural accessions are now available with intraspecific variation, and next generation sequencing has been used to generate data on single nucleotide

polymorphisms (SNPs) from over 1,000 of these accessions as part of the 1001 genomes project[17]. 100s of different phenotypes have been analyzed in this collection such as flowering time, leaf shape and size, the ability to resist to pathogens, etc.[18]. In this study, we identified variation in ovule number per flower in a screen of 189 Arabidopsis accessions and conducted a Genome Wide Association Study (GWAS) to identify loci associated with the ovule number trait. Further analysis of two loci identified in our GWAS revealed that the *NEW ENHANCER of ROOT DWARFISM* (*NERD1*) and *OVULE NUMBER ASSOCIATED 2* (*ONA2*) genes participate in the determination of ovule number during Arabidopsis flower development. The discovery of new ovule number regulators in Arabidopsis has the potential to provide targets for the development of crop varieties with greater yield.

Results

Natural Variation in Ovule Number

We set out to identify new regulators of ovule number in Arabidopsis by taking advantage of phenotypic variation in naturally occurring accessions. We obtained 189 Arabidopsis accessions from the ABRC and assayed them for variation in ovule number (Table S1). Since ovule number can vary throughout the life cycle of the plant[19], we determined the average number of ovules from flowers 6-10 on the main stem of plants that were vernalized for 4 weeks and then grown in long days at 22˚C. Under these growth conditions, accessions displayed a remarkable diversity in ovule number per

flower, with a range of 39-82 ovules per flower (Fig. 1a, b). The commonly used reference accession, Col-0, falls in the middle of the range with an average ovule number of 63±3 ovules.

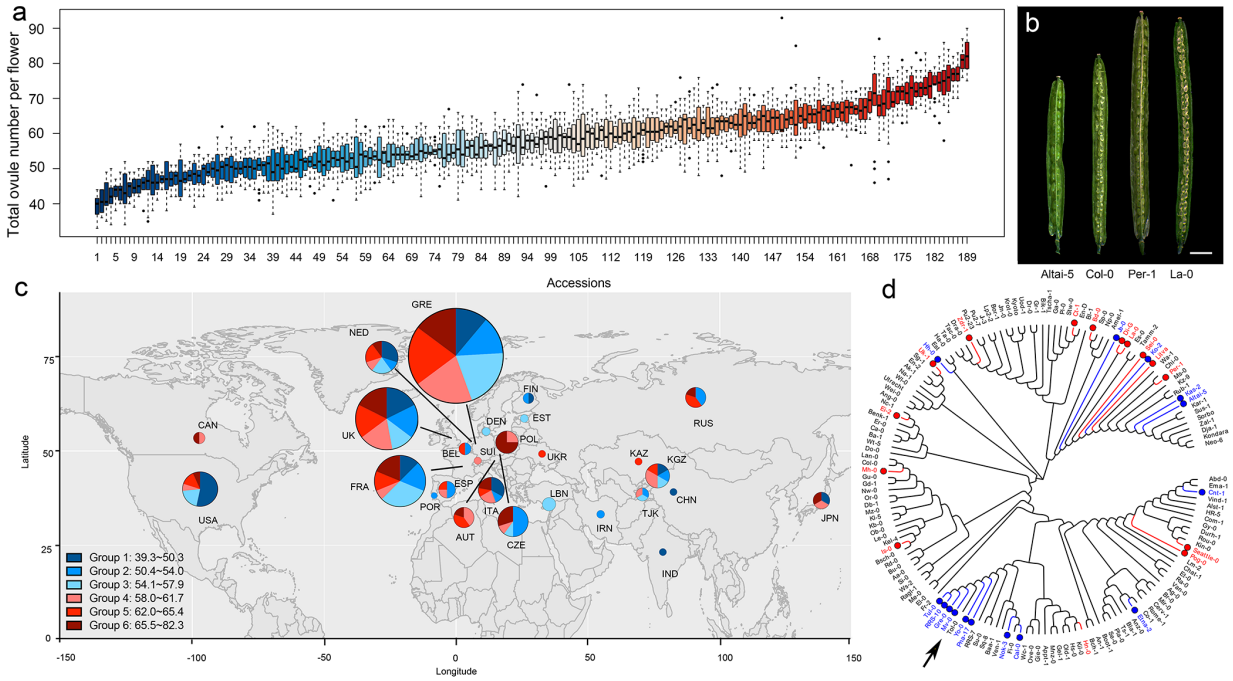

Figure 1. Arabidopsis accessions display natural variation in ovule number per flower. (**a**) Boxplot of ovule number in 189 Arabidopsis accessions. The detailed names of these accessions are in Supplementary Table 1. (**b**) Dissected siliques of low, medium, and high ovule number accessions (Bar=2.0mm). (**c**) Geographic distribution of accessions. Groups 1 to 6 correspond to ovule number ranking (from low to high), with the colors corresponding to panel A. The pie chart indicates the percentage of accessions in each country in each ovule number group, while the size of the pie chart corresponds to the total number of accessions per country. (**d**) Cladogram of accessions used in this study (generated in MEGA7). The 15 accessions labeled in blue had the lowest ovule numbers, and the 15 accessions labeled with red had the highest ovule numbers. The arrow points to a clade with clustered low ovule number accessions.

In contrast to flowering time variation which has been shown to correlate with latitude of origin in Arabidopsis accessions[20], ovule number was not strongly correlated with location of origin in the accessions analyzed (Fig. 1c, S1). Mapping ovule number data onto a cladogram of the accessions used in our study revealed a cluster of low ovule number accessions in one specific clade, indicating that these closely-related accessions may have similar genetic control of ovule number (Fig. 1d). Interestingly,

several clades were made up of accessions with high, medium, and low ovule numbers. This suggests that the ovule number trait may be regulated by different loci that have been selected for in some lineages.

GWAS reveals SNPs linked to natural variation in ovule number

In order to identify genomic regions linked to variation in ovule number, we assessed whether the average ovule number per flower from 148 accessions was predicted by Single Nucleotide Polymorphisms (SNP) available in the 1001 Full-sequence dataset; TAIR 9. Logarithmic transformation was applied to the ovule number data to make the results more reliable for parametric tests. Associations were tested for each SNP using a linear regression model (LM) and the results were analyzed using GWAPP[21] (Fig. 2a). A significance cutoff value of $-\log_{10}(p \text{ values}) \geq 6.2$ identified at least 9 genomic regions that are associated with variation in ovule number, while a higher cutoff of $-\log_{10}(p \text{ values}) \geq 7.5$ identifies only four significant genomic regions.

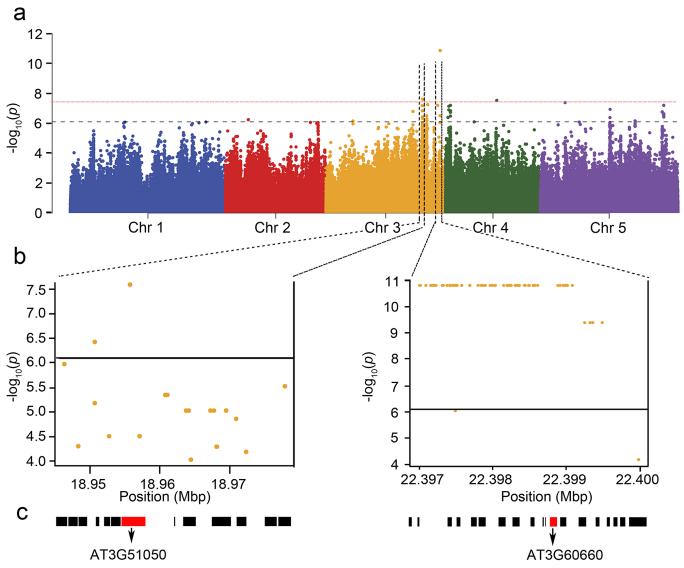

Figure 2. GWAS identifies candidate loci associated with ovule number per flower. (**a**) Manhattan plot for the SNPs associated with ovule number per flower. Chromosomes are depicted in different colors. The horizontal blue dashed line corresponds to a $-\log_{10}(p \text{ values}) \geq 6.2$ and the red dashed line corresponds to $-\log_{10}(p \text{ values}) \geq 7.5$ after Benjamini Hochberg (False Discovery Rate) correction. (**b**) The genomic region surrounding the two most significant GWA peaks on Chromosome 3. (**c**) Genes in the genomic region surrounding the two significant GWA peaks in (**b**). The red boxes are AT3G51050 (*NERD1*) and AT3T60660 (*ONA2*).

We next determined if known ovule number regulators (summarized in Cucinotta, 2014) colocalized with our GWAS loci. Only BIN2 mapped close to a significant association (Fig. S2). This indicates that our GWAS has identified novel functions for loci in the regulation of ovule number. For further analysis, we focused on the two loci with the lowest p-values which are both located on the long arm of chromosome 3 (Fig. 2b, c). Genes containing the most significantly associated SNPs as well as the 10 surrounding genes around the highest peak were considered as candidates for regulating ovule number. These genes were further prioritized based on whether they are expressed in developing pistils, by examining publicly available transcriptome data in ePlant[22] (Fig. S3). Based on this prioritization, 35 candidate genes were selected, and of these 26 insertion mutants were available from the Arabidopsis Biological Resource Center. All 26 mutants were evaluated for changes in ovule number compared to the wild-type background, Col-0 (Table S2). Of these, two had significantly reduced ovule number compared to the Col-0 control (Fig. 3a, S4). The strongest ovule number phenotype was found in insertion mutants in At3g51050, a gene that was recently identified in a screen for enhancers of exocyst-mediated root phenotypes and named *NEW ENHANCER OF ROOT DWARFISM 1* (*NERD1*)[23]. The second locus with T-DNA insertions affecting ovule number identified in our screen was At3g60660, which we call *OVULE NUMBER ASSOCIATED 2* (*ONA2)*. *ONA2* encodes an unknown protein containing a DUF1395 domain (TAIR) (Fig. 2c).

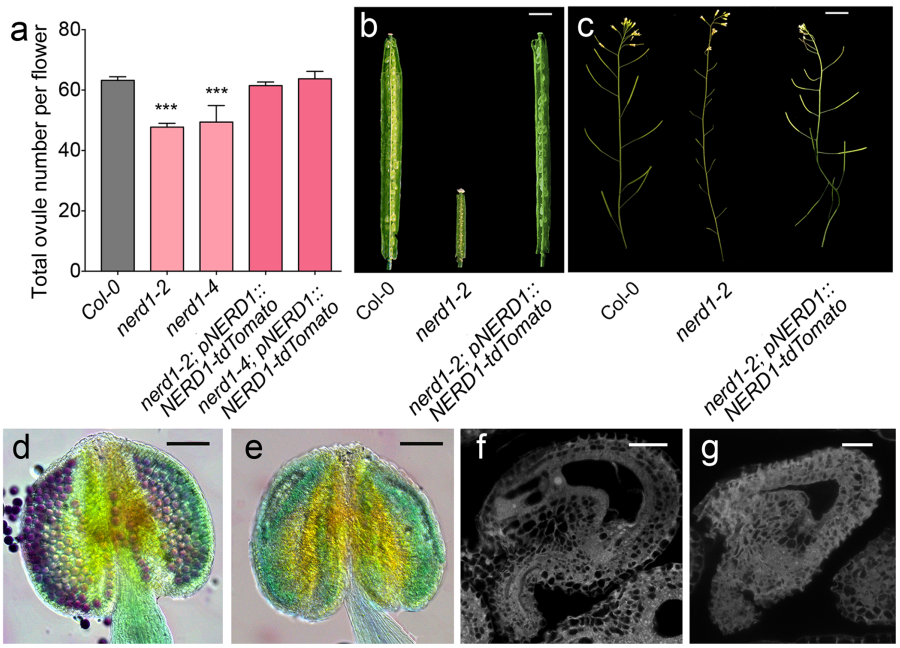

Figure 3. Reproductive phenotypes of *nerd1* mutants. (**a**) Bar graph of ovule number per flower in Col-0, *nerd1-2*, *nerd1-4* and their complementation lines. "***" indicates statistical significance (*p* value<0.001 determined by Student's t-test). (**b-c**) *nerd1-2/nerd1-2* displays lower ovule number, infertile ovules, and short siliques compared to Col-0 and complemented lines. (**d**) Alexander stained Col-0 anthers have viable pollen grains (red indicates viable pollen while the green is non-viable). (**e**) Alexander-stained *nerd1-2/nerd1-2* anthers have no viable pollen. (**f**) Col-0 mature ovule with a normal embryo sac. (**g**) *nerd1-2/nerd1-2* mature ovule with an aborted embryo sac.

NERD1 is a positive regulator of ovule number

We focused our analysis on *NERD1* since it had the strongest effect on ovule number. The fruits of homozygous mutants in two T-DNA insertion alleles (*nerd1-2* and *nerd1-4* described in [23]) had fewer ovules than wild-type plants (Fig. 3a). To confirm that this resulted from the disruption of NERD1, we generated transgenic plants expressing a translational fusion of the *NERD1* protein with the red-fluorescent protein tdTomato under the control of the native *NERD1* promoter. In *nerd1-2* and *nerd1-4* mutants, this transgene fully rescued the reduced ovule phenotype and resulted in plants with ovule numbers indistinguishable from Col-0 (Fig. 3a). This demonstrates that *NERD1* is a positive regulator of ovule number.

In addition to reduced ovule number per flower, homozygous *nerd1* mutants had fertility defects. Homozygous *nerd1-2* mutants had 100% unfertilized ovules and homozygotes of the less severe *nerd1-4* allele had 75% unfertilized ovules (Fig. 3b-c and S5). *nerd1-2* mutants displayed both male and female defects. No viable pollen grains were produced (Fig. 3d-e) and embryo sacs were often aborted, leading to 40% unfertilized ovules in *nerd1-2/nerd1-2* plants pollinated with wild-type pollen (Fig. 3f-g and S5). We performed reciprocal crosses between heterozygous *nerd1-2* mutants and Col-0 to determine if the fertility defects were gametophytic or sporophytic. When heterozygous *nerd1-2/NERD1* was used as the female, there was no transmission defect, demonstrating that the reduced female fertility in *nerd1-2* mutants was not gametophytic. When *nerd1-2/NERD1* was used as the pollen donor, the transmission efficiency of the mutant allele was reduced to 45%, indicating a male gametophytic transmission defect (Table 1).

Table 1. Transmission efficiency of the *nerd1-2* allele determined by reciprocal crosses with wild-type Col-0.

Female	Male	*NERD1/ NERD1*	*nerd1-2/ NERD1*	Female TE%	Male TE %
nerd1-2/NERD1	Col-0	43	42	97.67	NA
Col-0	*nerd1-2/NERD1*	92	41	NA	44.57

NERD1 encodes an integral membrane protein

Phylogenetic analyses indicate that *NERD1* is a member of a low-copy number, highly conserved gene family that is found throughout the plant kingdom and in cyanobacteria (Fig. 4a, b and [23]). The NERD1 protein is predicted to be an integral membrane protein

with a signal peptide and one transmembrane domain (Fig. 5a). The majority of the protein is predicted to be extracellular, with the transmembrane domain located near the C-terminus and a 17 amino acid cytoplasmic extension. Transient expression of a NERD1-GFP fusion in *Nicotiana benthamiana* with subcellular markers confirmed that NERD1 co-localizes with the Golgi marker and partially colocalizes with a plasma membrane marker (Fig. 5b and d). NERD1 does not co-localize with ER, peroxisome, and plastid markers (Fig. 5c and S6).

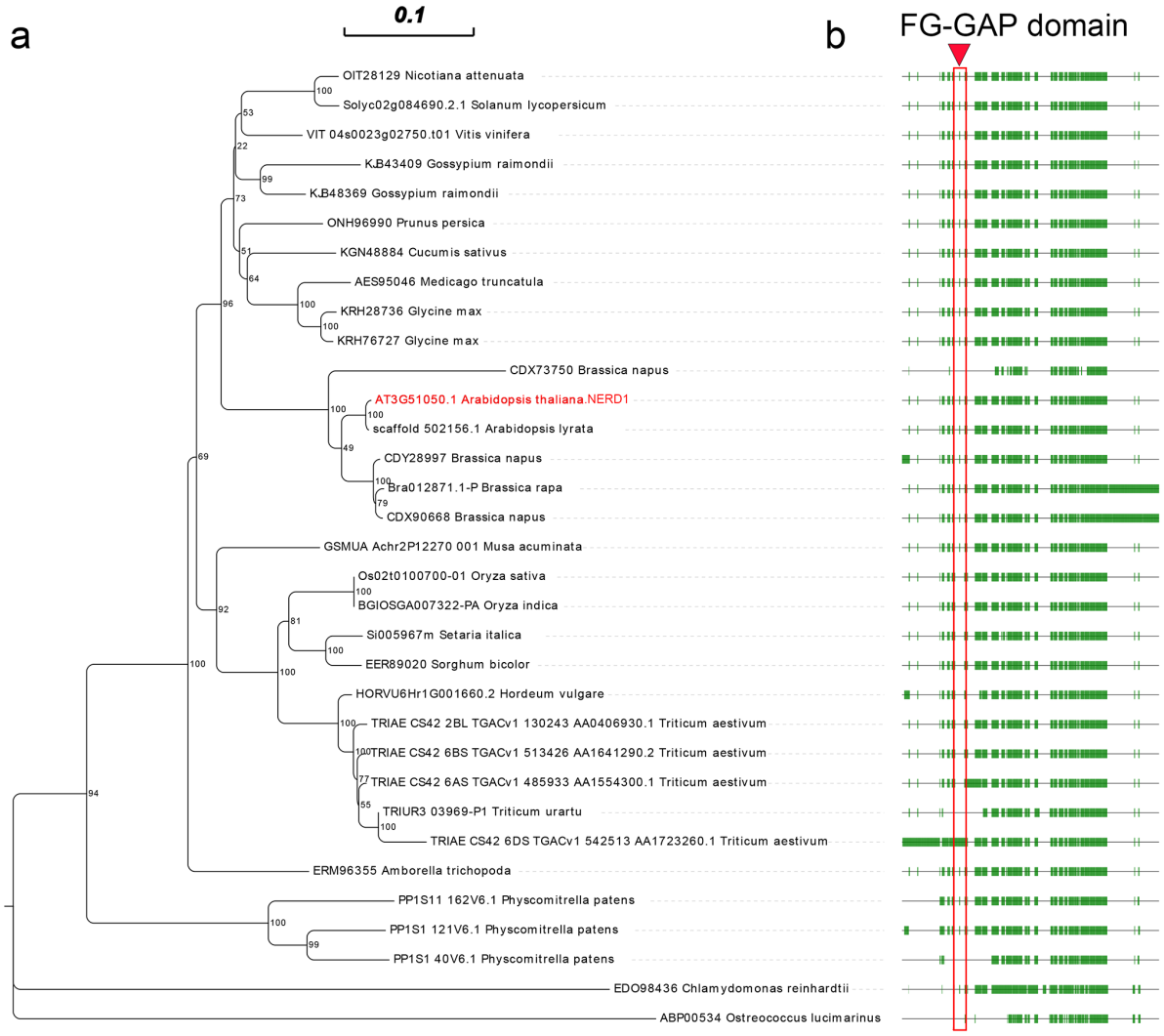

Figure 4. Phylogenetic tree for NERD1. (**a**) Phylogenetic tree from amino acid alignment of NERD1 generated using the Neighbor-joining method in MEGA7. (**b**) NERD1 alignment showing sequence conservation among species. The green boxes correspond to conserved regions of NERD1 and the lines represent gaps in the alignment. The red box indicates the FG-GAP domain annotated in NERD1 by Langhans, et al., 2017.

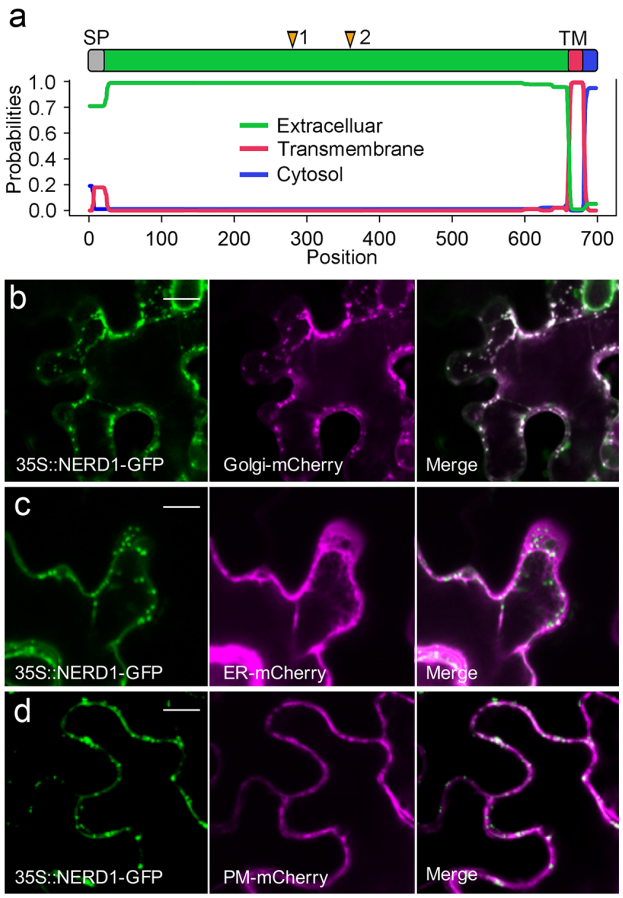

Figure 5. NERD1 co-localizes with a Golgi marker in *N. benthamiana* epidermal cells. (**a**) NERD1 protein domains determined by TMHMM 2.0. (**b**) NERD1-GFP (green signal) co-localizes with Golgi-mCherry (magenta signal) in *N. benthamiana* epidermal cells. (**c**) NERD1-GFP (green signal) does not co-localize with ER-mCherry (magenta signal). (**d**) NERD1-GFP (green signal) partially co-localizes with PM-mCherry (magenta signal). Bars=15 µm.

NERD1 is expressed throughout Arabidopsis development

The *nerd1* ovule number and fertility phenotypes suggest that *NERD1* should be expressed in developing flowers. We used a *NERD1*$_{pro}$*::gNERD1-GUS* fusion to examine *NERD1* expression throughout Arabidopsis development. In *NERD1*$_{pro}$*::gNERD1-GUS* inflorescences, GUS activity was detected throughout flower development, including inflorescences, developing and mature anthers, and in the

stigma, ovules, and carpel walls of mature pistils (Fig. 6). NERD1-GUS activity was present in the carpel margin meristem (CMM) in stage 9 flowers, where ovule initiation occurs (Fig. 6c and e). *NERD1* reporter expression in the CMM during pistil development is consistent with a role for *NERD1* in ovule initiation. During seedling development, the *NERD1-GUS* reporter was detected in shoot and root apical meristems (SAM and RAM) and in the vasculature (Fig. 6i).

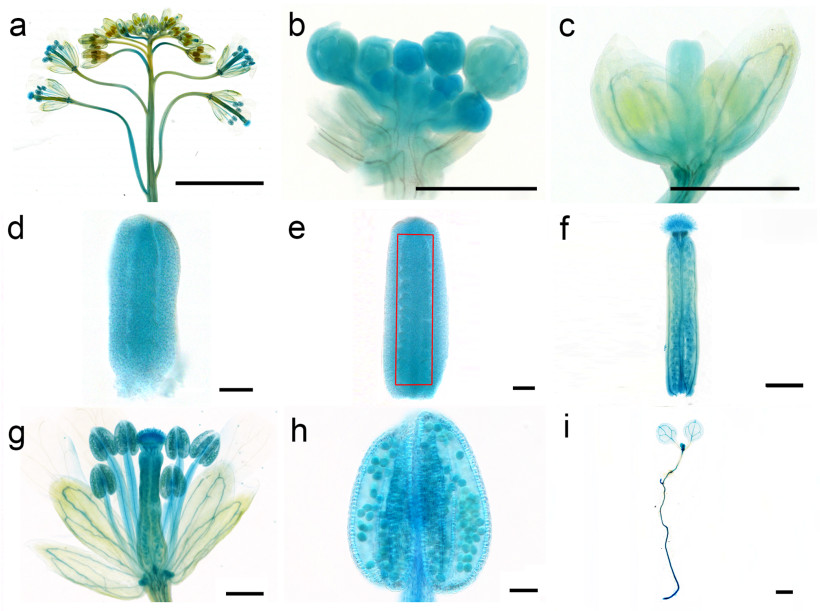

Figure 6. NERD1 expression in plant development. The NERD1$_{pro}$::NERD1-GUS reporter (blue signal) is detected in inflorescence (**a**-**b**), the flower in stage 9 (**c**), the pistil in stage 8 (**d**), the pistil in stage 9 (**e**), mature pistil (**f**), mature flower (**g**), mature anther (**h**), and SAM and RAM of seedlings (**i**).

Overexpression of NERD1 increases plant productivity

We examined *NERD1* transcript levels in the low ovule number accession Altai-5 compared to Col-0. *NERD1* transcript accumulation was reduced in Altai-5 buds as compared to Col-0 but similar in Altai-5 and Col-0 leaves (Fig. 7). We hypothesized that the low ovule number in Altai-5 may be linked to reduced *NERD1* expression in developing flowers.

In order to determine whether increasing *NERD1* expression is sufficient to increase ovule number, we transformed Col-0 and the low ovule number accession Altai-5, with a *NERD1-GFP* fusion construct driven by the constitutively expressed Cauliflower Mosaic Virus 35S promoter (*35S::NERD1-GFP*). Overexpression of *NERD1* had no effect on ovule number in the Col-0 background, but significantly increased ovule number in the Altai-5 background (Fig. 8a-c), indicating that the *NERD1* effect on ovule number is background-dependent. The *35S::NERD1-GFP* plants displayed an even more striking phenotype when overall plant architecture was examined (Fig. 8a). In both the Altai-5 and Col-0 backgrounds, *NERD1* overexpression led to increased branching (Fig. 8d) and shortened internode lengths between flowers, leading to an overall increase in flower number in the overexpression plants compared to untransformed controls (Fig. 8e-h). Thus, *NERD1* overexpression leads to increased biomass and reproductive capacity, with up to a 2.5-fold increase in total flower number over the lifespan of the plant. While all independent transformants displayed increased branching and flower number, some of the *35S::NERD1* plants were male sterile (Fig. S7). This male sterility correlated with *NERD1* expression levels and plants with higher *NERD1* transcript levels had more severe male sterility (Fig. S7). The sterility effect was more severe in Col-0 than in Altai-5 (Fig. S7). The lower endogenous *NERD1* expression in Altai-5 inflorescences might explain the lower

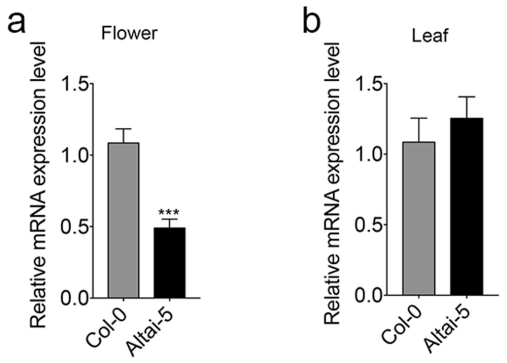

Figure 7. NERD1 expression is reduced in developing flowers of a low ovule number accession.
(**a**) qRT-PCR of NERD1 in Col-0 and Altai-5 inflorescences. (**b**) qRT-PCR of NERD1 in Col-0 and Altai-5 leaves. "***" indicates statistical significance at *p* value<0.001 determined by Student's t-test.

sensitivity of Altai-5 to *NERD1* overexpression with respect to male fertility, demonstrating background-dependent sensitivity to *NERD1* levels for both ovule number and male sterility.

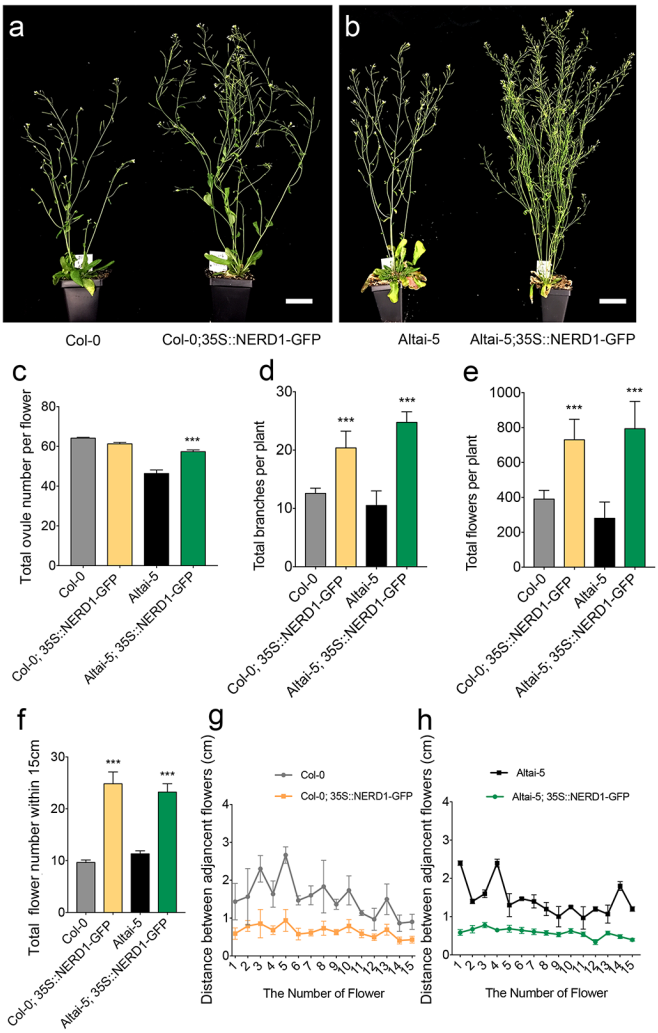

Figure 8. Overexpression of NERD1 affects plant architecture and fertility. (**a-b**) 35S::NERD1-GFP expressed in Col-0 and Altai-5 backgrounds. Bars=5cm. Bar graphs of total ovule number per flower (**c**), total branch number (**d**), total flower number per plant (**e**), number of flowers within 15 cm of the main shoot (**f**), and distance between adjacent flowers (**g-h**) in 35S::NERD1-GFP

NERD1 was recently identified in enhancer screen performed on exocyst mutants with weakly dwarfed roots. *nerd1* mutants have reduced root growth as a result of impaired cell expansion, indicating that NERD1 may be a positive regulator of exocyst-dependent root growth[23]. Consistently, the *35S::NERD1-GFP* plants had longer roots compared to

the Col-0 control, indicating that root development is also sensitive to *NERD1* expression levels (Fig. S8).

We compared the sequence of the *NERD1* locus in the 16 highest and 16 lowest ovule number accessions from our screen (Fig. 9a, S9). A non-synonymous SNP (C to A change in comparison to Col-0 reference) causing a Serine to Tyrosine change at amino acid 230 of NERD1 was present in 10 out of the 16 lowest ovule number accessions and not present in the 16 highest ovule number accessions (Fig. 9a). Across all of the accessions in our panel, the “A” allele at this position was significantly associated with lower ovule numbers (Fig. 9b). However, some accessions with the “C” allele of *NERD1* have low ovule numbers, including the Altai-5 accession, underscoring that multiple mechanisms influence ovule number in Arabidopsis (Fig. 9b).

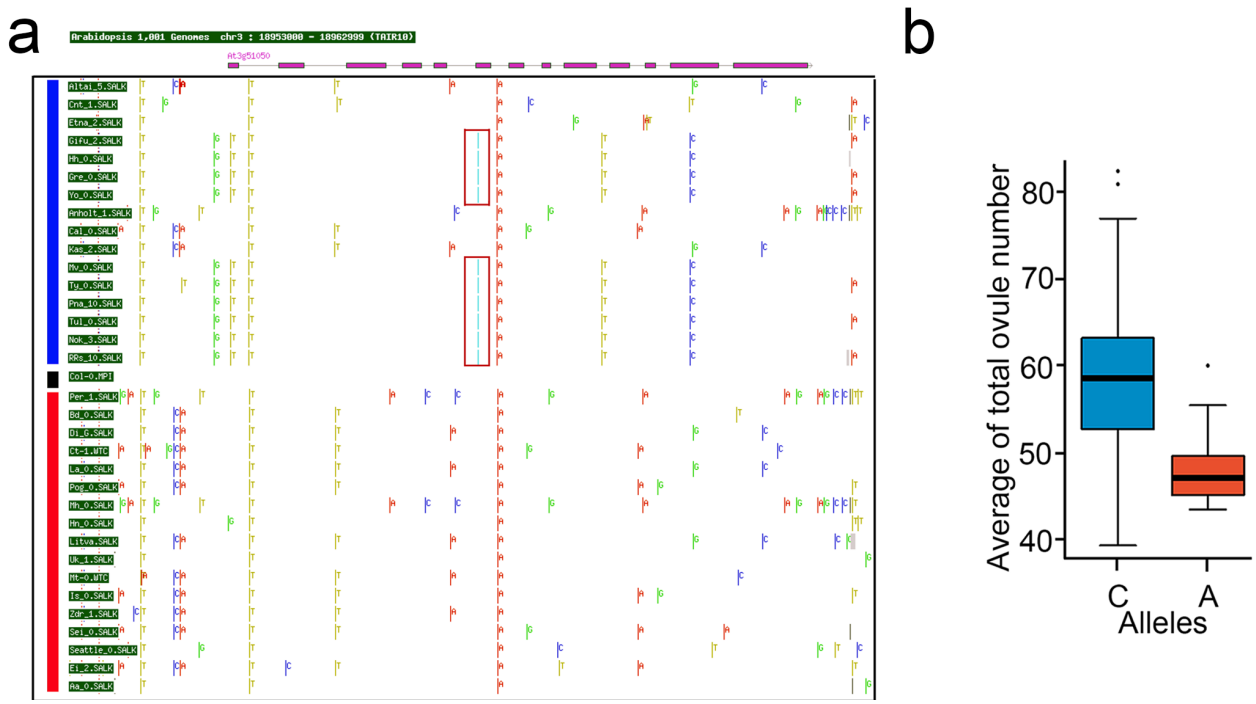

Figure 9. Sequence variation in the *NERD1* locus. (**a**) SNPs in and around the *NERD1* gene. The blue line indicates the 16 lowest ovule number accessions and the red line indicates the 16 highest ovule number accessions. SNPs are identified based on comparison to the Col-0 reference genome. The red boxes highlight low-ovule number associated SNPs (the turquoise bar indicates two SNPs in adjacent nucleotides, a non-synonymous C-A SNP and a synonymous C-G SNP). Only genomes that were available on the SALK 1,001 genomes browser (http://signal.salk.edu/atg1001/3.0/gebrowser.php) were considered. (**b**) Average ovule number within *NERD1* A and C allele-containing accessions.

Discussion

Our experiments revealed that Arabidopsis displays a wide variation in the number of ovules per flower, a key component of plant fitness and crop yield. Association genetics linked this natural variation to the plant-specific gene, *NERD1*, that regulates the number of ovules produced in Arabidopsis flowers and gametophyte development (Fig. 3) and was previously found to alter root growth[23]. Overexpression of *NERD1* led to dramatic effects on plant architecture, indicating that *NERD1* may be involved in regulating meristem activity during Arabidopsis development.

GWAS reveals new ovule number-associated loci in Arabidopsis

A quantitative trait locus (QTL) mapping study utilizing variation between L*er* and Cvi identified QTLs residing on chromosomes 1, 2 (near the *ERECTA* gene), and two QTL on chromosome 5[24]. No follow-up study has identified the genes underlying these QTLs. Our population displayed a much larger range of ovule numbers per flower (39-84) than that seen in Cvi vs L*er* (66 and 56, respectively). We identified 9 significant associations in our GWAS, but only one potentially overlaps with an ovule number QTL (see chromosome 5 in Fig. S2). Of the genes with an identified effect on ovule number, only BIN2 overlapped with a GWAS peak, indicating that our study has revealed at least seven novel regulators of ovule number in Arabidopsis. We molecularly identified two new genes that control ovule number that were linked to two GWAS peaks on chromosome 3. This expands that number of known ovule number determinants and confirms the value of GWAS as a forward genetics tool.

NERD1 may transmit signals across membranes

NERD1 is a plant-specific, low copy number gene that is found throughout the plant kingdom. NERD1 was recently identified as an enhancer of root development phenotypes in weak mutants of the exocyst subunits SEC8 and EXO70A1[23] While a direct interaction with the exocyst could not be identified, the authors identified Golgi localization of NERD1. Our GFP localization experiments confirmed Golgi localization but also identified fluorescence in the plasma membrane. In Arabidopsis, the NERD1 protein is predicted to encode a 698 amino acid protein with a signal peptide, one transmembrane domain, and a short (17 amino acid) cytoplasmic tail at the C-terminus. This topology is consistent with NERD1 being involved in transducing signals from the outside of the cell to the inside, perhaps as part of a complex with other membrane proteins. In animals, α-integrins and β-integrins share a similar topology with NERD1 and interact with each other to transduce information from the extracellular matrix to the inside of the cell[25]. The existence of integrin-like complexes in plants remains controversial, since plants lack proteins with clear sequence homology to animal integrins. However, antibodies to animal β-integrins interact with plant proteins, indicating structural conservation[26]. NERD1 has a predicted beta-propeller with a calcium-binding pocket similar to α-integrins in its extracellular domain[23], but determination of whether NERD1 functions in an integrin-like fashion awaits further investigation.

A second possibility is that NERD1 interacts with other types of proteins to transduce signals. In plants, receptor-like proteins (RLPs) with short cytoplasmic domains have

been shown to heterodimerize with receptor-like kinases (RLKs) to form a receptor complex that transduces extracellular signals to intracellular signaling networks. The Arabidopsis genome contains 57 RLPs with Leucine Rich Repeats (LRRs) in their extracellular domains[27]. These LRR-RLPs have a transmembrane domain near the C-terminus and a short cytoplasmic domain and are predicted to form complexes with LRR-RLKs. LRR-RLP/LRR-RLK complexes have been implicated in plant growth and development and plant immunity (reviewed in[28]). For example, the CLAVATA2 (CLV2) RLP forms a complex with the RLKs CORYNE (CRN) and/or CLAVATA1 (CLV1) RLK to perceive the CLAVATA3 (CLV3) ligand and trigger intracellular signaling related to shoot apical meristem maintenance[29-31]. Likewise, the TOO MANY MOUTHS (TMM) RLP interacts with the LRR-RLKs ERECTA (ER) and ERECTA-LIKE1 (ERL) to regulate stomatal patterning[32,33]. In contrast to the LRR-RLPs, NERD1 does not share sequence homology with other proteins in the Arabidopsis genome. Distinguishing whether NERD1 functions similarly to RLPs, integrins, or some other signaling network will require identification of NERD1-interacting proteins in future work.

NERD1 **and fertility**

Homozygous *nerd1* mutants are completely male sterile are partially female sterile. This sterility is due to a lack of pollen production and problems in female gametophyte development leading to aborted embryo sacs. Transmission efficiency tests using heterozygous loss-of-function mutants revealed that *nerd1* could be transmitted through the egg at near 100% efficiency, indicating a sporophytic effect on female gametophyte development. Ovule development mutants that have defective integument development

such as *short integuments 1* (*sin1*), *bell 1* (*bel1*) and *ant* fail to produce functional female gametophytes, indicating that female gametophyte development is dependent on properly differentiated sporophytic cells in the ovule[34-38]. Sporophytic development in ovules seem to be normal in *nerd1* mutants, yet embryo sacs abort. As a membrane protein, NERD1 could transmit some unknown signal between sporophytic and gametophytic cells during embryo sac development.

The male fertility defect in *nerd1* plants is more severe than the female defect. Homozygous *nerd1* anthers are empty, indicating that pollen development is not initiated or aborted very early. Transmission efficiency tests using pollen from heterozygous *nerd1* plants crossed to wild-type females revealed that *nerd1* also has gametophytic effects on pollen function. The sporophytic effects could be related to early stages of anther development. In particular, specification of the tapetum is critical for pollen development (reviewed in[39]). In our *35S::NERD1* experiment, transformants that accumulated the most *NERD1* transcripts were male sterile. Together these results indicate that pollen development is sensitive to *NERD1* levels, i.e. either too much or too little *NERD1* is detrimental to pollen development. Future experiments should focus on determining the stage of anther and/or pollen development that is affected in *nerd1* mutants and the specific cell types that express *NERD1* in developing anthers.

Even though *NERD1* is expressed broadly throughout the plant, above ground vegetative development appears to be normal in *nerd1* loss-of-function mutants. However, *nerd1* roots are shorter than normal and have root hair defects that include

bulging and rupture[23]. *NERD1* could have distinct or related developmental functions in roots and flowers, as is seen for many of the genes involved in hormonal regulation of development[40].

NERD1 **regulates lateral organ formation**

NERD1 overexpression under control of the 35S promoter dramatically changed plant architecture in both the Col-0 and Altai-5 backgrounds. *NERD1* overexpression plants produced significantly more branches than wild-type controls and produced significantly more flowers that were produced at closer intervals along the stem. Like branches and flowers, ovules are lateral organs produced from meristematic cells, indicating that *NERD1* may be a positive regulator of meristem activity. Lateral meristem activation and subsequent branching have been shown to be affected by several different hormones (reviewed in[41]). Classic experiments in *Vicia faba* showed that auxin produced in the shoot apex inhibits axillary meristems[42], and more recently strigolactones were identified as graft-transmissible suppressors of branching (reviewed in [43]). Gibberellins also repress shoot branching in Arabidopsis, maize, and rice, with GA-deficient mutants displaying increased branching compared to wild-type controls[44-47]. In contrast, cytokinins and brassinosteroids are both positive regulators of branching[46-50]. The mechanism through which these plant hormones work together to regulate branching is unknown, but auxin has been proposed to control cytokinin and strigolactone biosynthesis[51,52], while the brassinosteroid signaling regulator *BES1* may inhibit strigolactone signaling to promote branching[53]. The promotion of branching in *35S::NERD1* plants could be related to regulation of one or more of these hormonal

pathways. Like *NERD1*, upregulation of both cytokinin and brassinosteroid signaling pathways have been shown to positively regulate branching and ovule number[15,50,53,54], suggesting that *NERD1* may be intimately connected to these pathways. Future research is needed to explore the intersection between *NERD1* and hormonal pathways.

***NERD1*-induced increases in ovule number are background-dependent**

Overexpression of *NERD1* in the Col-0 and Altai-5 backgrounds led to increased branching and flower number, but ovule number was only increased in the Altai-5 background, suggesting a background-dependence on the ovule number trait. In Arabidopsis, natural accessions were shown to respond differently in their ability to buffer GA perturbations caused by overexpressing GA20 oxidase 1, which encodes a rate-limiting enzyme for GA biosynthesis[55]. Genetic background dependence has been shown to be a wide-spread phenomenon in *C. elegans*, with approximately 20% of RNAi-induced mutations (out of 1400 genes tested) displaying different phenotypic severity in two different genetic backgrounds[56]. Similar to our results with *NERD1*, where Altai-5 has lower endogenous levels of the *NERD1* transcript in developing flowers compared to Col-0, the severity of the *C. elegans* phenotypes could be linked to gene expression levels of either the target gene itself or other genes in the same pathway[56].

Our GWAS revealed multiple novel loci that control ovule number in Arabidopsis. It remains to be seen if exocyst function is linked to NERD1's role in ovule number

determination. Identification of NERD1 interacting proteins will provide candidates for other players in the NERD1 pathway. Some of the other novel loci identified in our GWAS may well participate in the same signaling pathway as *NERD1*. While *NERD1* is a promising candidate for engineering plants with increased ovule number, the differential responses to *NERD1* overexpression seen in Altai-5 and Col-0 suggest that specific alleles at other loci may be necessary for achieving maximum effect of *NERD1* overexpression.

Materials and Methods

Plant Material and Growth Conditions

Arabidopsis thaliana accessions and insertion mutants were ordered from the Arabidopsis Biological Resource Center (Ohio State University). Seeds were sterilized and plated on ½ Murashige and Skoog (MS) plates. All plates were sealed and stratified at 4 ˚C for two days, and then transferred to the growth chamber (long day conditions, 16h of light and 8 h of dark at 22˚C) for germination and growth. After one-week, seedlings were transplanted to soil. Many of the Arabidopsis accessions require vernalization for flowering[57], we therefore chose to vernalize all of the accessions in our study for 4 weeks at 4 ˚C. After vernalization, the plants were returned to the growth chamber and grown under the long day conditions described above.

Seeds from transformed lines were sterilized and plated on ½ MS plate with 20mg/L hygromycin for selection of transgenic seedlings, which were then transplanted to soil and grown in long days.

Ovule Number Phenotyping

For determination of ovule number per flower, we counted four to five siliques per plant and five plants per accession. Carpel walls were removed with a dissecting needle and total ovule number (including unfertilized and aborted ovules) was counted with the aid of a Leica dissecting microscope. To minimize age-related variation in ovule number, we counted siliques from flowers 6-10 on the primary shoot for all accessions.

Genome-Wide Association Study

GWAS was performed using GWAPP, which is a GWAS web application for Genome-Wide Association Mapping in *Arabidopsis* (http://gwas.gmi.oeaw.ac.at) [21]. In our study, 148 accessions had single nucleotide polymorphisms (SNPs) data available on the 1001 Full-sequence dataset; TAIR 9. Logarithmic transformation was applied to make the results more reliable for parametric tests. A simple linear regression (LM) was used to generate the Manhattan plot by using GWAPP[21]. SNPs with P values $\leq 1 \times 10^{-6}$ were further considered as candidate loci linked to alleles that regulate ovule number (a horizontal dashed line in Fig. 2 shows the 5% FDR threshold $-\log_{10}p$ value=6.2, which was computed by the Benjamini-Hochberg-Yekutieli method). SNPs with <15 minor allele count (MAC) were not considered to help control false positive rates. 10 genes flanking the highest SNP for each locus were tabulated as candidate genes for each significant association.

Cloning and Generation of Transgenic Lines

For complementation and overexpression experiments, Gateway Technology was used

to make all the constructs. Genomic DNA fragments corresponding to the coding regions of candidate genes were amplified from either beginning of the promoter (defined by the end of the upstream gene) or the start codon to the end of the CDS (without stop codon) by PCR with primers that had attB1 and attB2 sites from Col-0 genomic DNA (see supplementary table 3 for primer sequences). For amplifying At3g60660 and At3g51050, PHUSION High-Fidelity Polymerase (NEB, M0535S) was used. All the PCR products were put into entry vector pDONR207 by BP reactions and then were recombined into destination vector pMDC83 (GFP) by LR reaction[58]. Native promoter constructs were amplified from ~2KB promoter region to the end (without stop codon) by PCR with primers that had attB1 and attB2 sites from Col-0 genomic DNA. The PCR products were put into entry vector pDONR207 by BP reactions and then were recombined into destination vector pMDC32 (tdTomato) and pMDC163 (GUS) by LR reaction. All constructs were transformed into *Agrobacterium tumefaciens* strain GV3101 and then used for plant transformation by the floral-dip method[59].

GUS Staining

GUS staining was performed as previously described[60]. Samples were imaged with Differential Interference Contrast (DIC) on a Nikon Eclipse Ti2-E microscope. 12 independent T1 NERD-GUS transformants were analyzed and showed similar GUS patterns.

Transient Expression in *N. benthamiana*

Leaves from 3-4 week old *N. benthamiana* were co-infiltrated with 35S::NERD1-GFP

and Golgi-mCherry, ER-mCherry, PM-mCherry, Plastid- mCherry and Peroxisome-mCherry markers from[61] as previously described[62]. Leaves were imaged 2-3 days after infiltration with a Nikon A1Rsi inverted confocal microscope under 20x dry and 40x water objectives with GFP excited by a 488nm laser and mCherry excited by a 561nm laser in normal mode.

Alexander Staining of Pollen

Mature anthers from Col-0 and *nerd1-2/nerd1-2* were dissected under the Leica dissecting microscope and placed into a drop (20 µl) of Alexander staining solution on a microscope slide[63]. After several minutes of staining, samples were imaged with a Nikon Eclipse Ti2-E microscope.

Quantitative Real-time RT-PCR

For qRT-PCR, leaves and young flowers were collected from mature plants of Col-0 and Altai-5. Samples were immediately frozen in liquid nitrogen, ground, and total RNA was extracted using the E.Z.N.A Plant RNA kit (OMEGA, USA). Oligo-dT primers and Superscript II reverse transcriptase (Invitrogen) was used for cDNA synthesis. qRT-PCR reactions were prepared using SYBR Green PCR Master Mix and PCR was conducted with a StepOnePlus RT-PCR system. Relative quantifications were performed for all genes with the Actin11 used as an internal reference. The primers used for qRT-PCR shown in supplementary table 3.

Phylogenetic Analysis

The cladogram tree was generated in MEGA7, which nucleotide distance and neighbor-join tree file were calculated by PHYlogeny Inference Package (PHYLIP, version 3.696). The phylogenetic tree of NERD1 was inferred using neighbor-joining method in MEGA7[64]. The associated taxa clustered together with the bootstrap test (1000 replicates)[65]. All the branch lengths are in the same units as those of the evolutionary distances used to generate the phylogenetic tree.

Figure Legends

Figure 1. Arabidopsis accessions display natural variation in ovule number per flower. (**a**) Boxplot of ovule number in 189 Arabidopsis accessions. The detailed names of these accessions are in Supplementary Table 1. (**b**) Dissected siliques of low, medium, and high ovule number accessions (Bar=2.0mm). (**c**) Geographic distribution of accessions. Groups 1 to 6 correspond to ovule number ranking (from low to high), with the colors corresponding to panel A. The pie chart indicates the percentage of accessions in each country in each ovule number group, while the size of the pie chart corresponds to the total number of accessions per country. (**d**) Cladogram of accessions used in this study (generated in MEGA7). The 15 accessions labeled in blue had the lowest ovule numbers, and the 15 accessions labeled with red had the highest ovule numbers. The arrow points to a clade with clustered low ovule number accessions.

Figure 2. GWAS identifies candidate loci associated with ovule number per

flower. (**a**) Manhattan plot for the SNPs associated with ovule number per flower. Chromosomes are depicted in different colors. The horizontal blue dashed line corresponds to a $-\log_{10}(p \text{ values}) \geq 6.2$ and the red dashed line corresponds to $-\log_{10}(p \text{ values}) \geq 7.5$ after Benjamini Hochberg (False Discovery Rate) correction. (**b**) The genomic region surrounding the two most significant GWA peaks on Chromosome 3. (**c**) Genes in the genomic region surrounding the two significant GWA peaks in (**b**). The red boxes are AT3G51050 (*NERD1*) and AT3T60660 (*ONA2*).

Figure 3. Reproductive phenotypes of *nerd1* mutants. (**a**) Bar graph of ovule number per flower in Col-0, *nerd1-2*, *nerd1-4* and their complementation lines. "***" indicates statistical significance (*p* value<0.001 determined by Student's t-test). (**b**-**c**) *nerd1-2/nerd1-2* displays lower ovule number, infertile ovules, and short siliques compared to Col-0 and complemented lines. (**d**) Alexander stained Col-0 anthers have viable pollen grains (red indicates viable pollen while the green is non-viable). (**e**) Alexander-stained *nerd1-2/nerd1-2* anthers have no viable pollen. (**f**) Col-0 mature ovule with a normal embryo sac. (**g**) *nerd1-2/nerd1-2* mature ovule with an aborted embryo sac. Bars=2.5mm (**b**-**c**), 20μm (**d**-**g**).

Figure 4. Phylogenetic tree for NERD1. (**a**) Phylogenetic tree from amino acid alignment of NERD1 generated using the Neighbor-joining method in MEGA7. (**b**) NERD1 alignment showing sequence conservation among species. The green boxes correspond to conserved regions of NERD1 and the lines represent gaps in the

alignment. The red box indicates the FG-GAP domain annotated in NERD1 by Langhans, et al., 2017.

Figure 5. NERD1 co-localizes with a Golgi marker in *N. benthamiana* epidermal cells. (**a**) NERD1 protein domains determined by TMHMM 2.0. (**b**) NERD1-GFP (green signal) co-localizes with Golgi-mCherry (magenta signal) in *N. benthamiana* epidermal cells. (**c**) NERD1-GFP (green signal) does not co-localize with ER-mCherry (magenta signal). (**d**) NERD1-GFP (green signal) partially co-localizes with PM-mCherry (magenta signal). Bars=15 μm.

Figure 6. NERD1 expression in plant development. The $NERD1_{pro}$::NERD1-GUS reporter (blue signal) is detected in inflorescence (**a**-**b**), the flower in stage 9 (**c**), the pistil in stage 8 (**d**), the pistil in stage 9 (**e**), mature pistil (**f**), mature flower (**g**), mature anther (**h**), and SAM and RAM of seedlings (**i**). Bars=25 μm.

Figure 7. NERD1 expression is reduced in developing flowers of a low ovule number accession.

(**a**) qRT-PCR of NERD1 in Col-0 and Altai-5 inflorescences. (**b**) qRT-PCR of NERD1 in Col-0 and Altai-5 leaves. "***" indicates statistical significance at p value<0.001 determined by Student's t-test.

Figure 8. Overexpression of NERD1 affects plant architecture and fertility. (**a**-**b**) 35S::NERD1-GFP expressed in Col-0 and Altai-5 backgrounds. Bars=5cm. Bar graphs

of total ovule number per flower (**c**), total branch number (**d**), total flower number per plant (**e**), number of flowers within 15 cm of the main shoot (**f**), and distance between adjacent flowers (**g**-**h**) in 35S::NERD1-GFP transformants in the Col-0 and Altai-5 backgrounds compared to untransformed controls.

Figure 9. Sequence variation in the *NERD1* locus. (**a**) SNPs in and around the *NERD1* gene. The blue line indicates the 16 lowest ovule number accessions and the red line indicates the 16 highest ovule number accessions. SNPs are identified based on comparison to the Col-0 reference genome. The red boxes highlight low-ovule number associated SNPs (the turquoise bar indicates two SNPs in adjacent nucleotides, a non-synonymous C-A SNP and a synonymous C-G SNP). Only genomes that were available on the SALK 1,001 genomes browser (http://signal.salk.edu/atg1001/3.0/gebrowser.php) were considered. (**b**) Average ovule number within *NERD1* A and C allele-containing accessions.

Supplemental Material

Supplementary Figure 1. Statistical analysis of the association between geographic distribution and ovule number per flower in the Arabidopsis accessions used in the GWAS.

Supplementary Figure 2. Previously identified ovule number related genes' position in relation to the Manhattan plot generated from the ovule number GWAS.

Supplementary Figure 3. Heat map of candidate gene expression patterns in reproductive tissues.

Supplementary Figure 4. Average ovule number per flower of candidate gene T-DNA mutants on chromosome 3.

Supplementary Figure 5. Homozygous *nerd1* mutants have high levels of infertility can be partially rescued by pollinating with Col-0 wild-type pollen.

Supplementary Figure 6. Co-localization of 35S::NERD1-GFP with peroxisome and plastid markers.

Supplementary Figure 7. Male sterility in *35S::NERD1* plants is linked to high *NERD1* expression.

Supplementary Figure 8. *NERD1* is involved in in root growth.

Supplementary Figure 9. Amino acid changes in and around the *NERD1* gene in low and high ovule number accessions.

Supplementary table 1. List of Arabidopsis accessions used in the study and their ovule number data.

Supplementary Figure 2. Chromosome 3 candidate genes and insertion mutants.

Supplementary Figure 3. List of primers used for genotyping and cloning.

References

1. Palmer, R.G., Albertsen, M.C. & Heer, H. Pollen production in soybeans with respect to genotype, environment, and stamen position. *Euphytica* **27**, 427-433 (1978).
2. Uribelarrea, M., Cárcova, J., Otegui, M.E. & Westgate, M.E. Pollen Production, Pollination Dynamics, and Kernel Set in Maize. *Crop Science* **42**, 1910-1918 (2002).
3. Yan, J. *et al.* Arabidopsis Pollen Fertility Requires the Transcription Factors CITF1 and SPL7 That Regulate Copper Delivery to Anthers and Jasmonic Acid Synthesis. *Plant Cell* **29**, 3012-3029 (2017).
4. Coen, E.S. & Meyerowitz, E.M. The war of the whorls: genetic interactions controlling flower development. *Nature* **353**, 31-7 (1991).

5. Smyth, D.R., Bowman, J.L. & Meyerowitz, E.M. Early Flower Development in Arabidopsis. *Plant Cell* **2**, 755-767 (1990).
6. Reyes-Olalde, J.I., Zuniga-Mayo, V.M., Chavez Montes, R.A., Marsch-Martinez, N. & de Folter, S. Inside the gynoecium: at the carpel margin. *Trends Plant Sci* **18**, 644-55 (2013).
7. Robinson-Beers, K., Pruitt, R.E. & Gasser, C.S. Ovule Development in Wild-Type Arabidopsis and Two Female-Sterile Mutants. *Plant Cell* **4**, 1237-1249 (1992).
8. Drews, G.N. & Koltunow, A.M. The female gametophyte. *Arabidopsis Book* **9**, e0155 (2011).
9. Cucinotta, M., Colombo, L. & Roig-Villanova, I. Ovule development, a new model for lateral organ formation. *Front Plant Sci* **5**, 117 (2014).
10. Klucher, K.M., Chow, H., Reiser, L. & Fischer, R.L. The AINTEGUMENTA gene of arabidopsis required for ovule and female gametophyte development is related to the floral homeotic gene APETALA2. *Plant Cell* **8**, 137-153 (1996).
11. Azhakanandam, S., Nole-Wilson, S., Bao, F. & Franks, R.G. SEUSS and AINTEGUMENTA mediate patterning and ovule initiation during gynoecium medial domain development. *Plant Physiology* **146**, 1165-1181 (2008).
12. Galbiati, F. *et al.* An integrative model of the control of ovule primordia formation. *Plant J* **76**, 446-55 (2013).
13. Nemhauser, J.L., Feldman, L.J. & Zambryski, P.C. Auxin and ETTIN in Arabidopsis gynoecium morphogenesis. *Development* **127**, 3877-3888 (2000).
14. Bencivenga, S., Simonini, S., Benkova, E. & Colombo, L. The transcription factors BEL1 and SPL are required for cytokinin and auxin signaling during ovule development in Arabidopsis. *Plant Cell* **24**, 2886-97 (2012).
15. Bartrina, I., Otto, E., Strnad, M., Werner, T. & Schmulling, T. Cytokinin regulates the activity of reproductive meristems, flower organ size, ovule formation, and thus seed yield in Arabidopsis thaliana. *Plant Cell* **23**, 69-80 (2011).
16. Huang, H.Y. *et al.* BR Signal Influences Arabidopsis Ovule and Seed Number through Regulating Related Genes Expression by BZR1. *Molecular Plant* **6**, 456-469 (2013).
17. Weigel, D. Natural variation in Arabidopsis: from molecular genetics to ecological genomics. *Plant Physiol* **158**, 2-22 (2012).
18. Atwell, S. *et al.* Genome-wide association study of 107 phenotypes in Arabidopsis thaliana inbred lines. *Nature* **465**, 627-31 (2010).
19. Wetzsteini, H.Y., Yi, W.G., Porter, J.A. & Ravid, N. Flower Position and Size Impact Ovule Number per Flower, Fruitset, and Fruit Size in Pomegranate. *Journal of the American Society for Horticultural Science* **138**, 159-166 (2013).
20. Stinchcombe, J.R. *et al.* A latitudinal cline in flowering time in Arabidopsis thaliana modulated by the flowering time gene FRIGIDA. *Proc Natl Acad Sci U S A* **101**, 4712-7 (2004).
21. Seren, U. *et al.* GWAPP: a web application for genome-wide association mapping in Arabidopsis. *Plant Cell* **24**, 4793-805 (2012).
22. Waese, J. *et al.* ePlant: Visualizing and Exploring Multiple Levels of Data for Hypothesis Generation in Plant Biology. *Plant Cell* **29**, 1806-1821 (2017).
23. Cole, R. *et al.* A Broadly-Conserved NERD Genetically Interacts with the Exocyst to Affect Root Growth and Cell Expansion. *Journal of Experimental Botany*, ery162-ery162 (2018).

24. Alonso-Blanco, C., Blankestijn-de Vries, H., Hanhart, C.J. & Koornneef, M. Natural allelic variation at seed size loci in relation to other life history traits of Arabidopsis thaliana. *Proc Natl Acad Sci U S A* **96**, 4710-7 (1999).
25. Barczyk, M., Carracedo, S. & Gullberg, D. Integrins. *Cell Tissue Res* **339**, 269-80 (2010).
26. Nagpal, P. & Quatrano, R.S. Isolation and characterization of a cDNA clone from Arabidopsis thaliana with partial sequence similarity to integrins. *Gene* **230**, 33-40 (1999).
27. Wang, G. *et al.* A genome-wide functional investigation into the roles of receptor-like proteins in Arabidopsis. *Plant Physiol* **147**, 503-17 (2008).
28. He, Y., Zhou, J., Shan, L. & Meng, X. Plant cell surface receptor-mediated signaling - a common theme amid diversity. *J Cell Sci* **131**(2018).
29. Bleckmann, A., Weidtkamp-Peters, S., Seidel, C.A. & Simon, R. Stem cell signaling in Arabidopsis requires CRN to localize CLV2 to the plasma membrane. *Plant Physiol* **152**, 166-76 (2010).
30. Brand, U., Fletcher, J.C., Hobe, M., Meyerowitz, E.M. & Simon, R. Dependence of Stem Cell Fate in Arabidopsis on a Feedback Loop Regulated by CLV3 Activity. *Science* **289**, 617-619 (2000).
31. Zhu, Y. *et al.* Analysis of interactions among the CLAVATA3 receptors reveals a direct interaction between CLAVATA2 and CORYNE in Arabidopsis. *Plant J* **61**, 223-33 (2010).
32. Abrash, E.B., Davies, K.A. & Bergmann, D.C. Generation of signaling specificity in Arabidopsis by spatially restricted buffering of ligand-receptor interactions. *Plant Cell* **23**, 2864-79 (2011).
33. Shpak, E.D., McAbee, J.M., Pillitteri, L.J. & Torii, K.U. Stomatal patterning and differentiation by synergistic interactions of receptor kinases. *Science* **309**, 290-3 (2005).
34. Elliott, R.C. *et al.* AINTEGUMENTA, an APETALA2-like gene of Arabidopsis with pleiotropic roles in ovule development and floral organ growth. *The Plant Cell* **8**, 155-168 (1996).
35. Klucher, K.M., Chow, H., Reiser, L. & Fischer, R.L. The AINTEGUMENTA gene of Arabidopsis required for ovule and female gametophyte development is related to the floral homeotic gene APETALA2. *The Plant Cell* **8**, 137-153 (1996).
36. Modrusan, Z., Reiser, L., Feldmann, K.A., Fischer, R.L. & Haughn, G.W. Homeotic Transformation of Ovules into Carpel-like Structures in Arabidopsis. *The Plant Cell* **6**, 333-349 (1994).
37. Robinson-Beers, K., Pruitt, R.E. & Gasser, C.S. Ovule Development in Wild-Type Arabidopsis and Two Female-Sterile Mutants. *The Plant Cell* **4**, 1237-1249 (1992).
38. Schneitz, K., Hulskamp, M., Kopczak, S.D. & Pruitt, R.E. Dissection of sexual organ ontogenesis: a genetic analysis of ovule development in Arabidopsis thaliana. *Development* **124**, 1367-1376 (1997).
39. Wilson, Z.A. & Zhang, D.B. From Arabidopsis to rice: pathways in pollen development. *J Exp Bot* **60**, 1479-92 (2009).
40. Schaller, G.E., Bishopp, A. & Kieber, J.J. The Yin-Yang of Hormones: Cytokinin and Auxin Interactions in Plant Development. *The Plant Cell* **27**, 44-63 (2015).
41. Rameau, C. *et al.* Multiple pathways regulate shoot branching. *Front Plant Sci* **5**, 741 (2014).

42. Thimann, K.V. & Skoog, F. Studies on the Growth Hormone of Plants: III. The Inhibiting Action of the Growth Substance on Bud Development. *Proc Natl Acad Sci U S A* **19**, 714-6 (1933).
43. Domagalska, M.A. & Leyser, O. Signal integration in the control of shoot branching. *Nature Reviews Molecular Cell Biology* **12**, 211 (2011).
44. Lo, S.F. *et al.* A novel class of gibberellin 2-oxidases control semidwarfism, tillering, and root development in rice. *Plant Cell* **20**, 2603-18 (2008).
45. Silverstone, A.L., Mak, P.Y., Martinez, E.C. & Sun, T.P. The new RGA locus encodes a negative regulator of gibberellin response in Arabidopsis thaliana. *Genetics* **146**, 1087-99 (1997).
46. Best, N.B. *et al.* nana plant2 Encodes a Maize Ortholog of the Arabidopsis Brassinosteroid Biosynthesis Gene DWARF1, Identifying Developmental Interactions between Brassinosteroids and Gibberellins. *Plant Physiol* **171**, 2633-47 (2016).
47. Best, N.B., Johal, G. & Dilkes, B.P. Phytohormone inhibitor treatments phenocopy brassinosteroid–gibberellin dwarf mutant interactions in maize. *Plant Direct* **1**(2017).
48. Wickson, M. & Thimann, K.V. The Antagonism of Auxin and Kinetin in Apical Dominance. *Physiologia Plantarum* **11**, 62-74 (1958).
49. Sachs, T. & Thimann, K.V. THE ROLE OF AUXINS AND CYTOKININS IN THE RELEASE OF BUDS FROM DOMINANCE. *American Journal of Botany* **54**, 136-144 (1967).
50. Yin, Y. *et al.* BES1 Accumulates in the Nucleus in Response to Brassinosteroids to Regulate Gene Expression and Promote Stem Elongation. *Cell* **109**, 181-191 (2002).
51. Foo, E. *et al.* The branching gene RAMOSUS1 mediates interactions among two novel signals and auxin in pea. *Plant Cell* **17**, 464-74 (2005).
52. Shimizu-Sato, S., Tanaka, M. & Mori, H. Auxin-cytokinin interactions in the control of shoot branching. *Plant Mol Biol* **69**, 429-35 (2009).
53. Wang, Y. *et al.* Strigolactone/MAX2-induced degradation of brassinosteroid transcriptional effector BES1 regulates shoot branching. *Dev Cell* **27**, 681-8 (2013).
54. Huang, H.Y. *et al.* BR signal influences Arabidopsis ovule and seed number through regulating related genes expression by BZR1. *Mol Plant* **6**, 456-69 (2013).
55. Nam, Y.J. *et al.* Natural Variation of Molecular and Morphological Gibberellin Responses. *Plant Physiol* **173**, 703-714 (2017).
56. Vu, V. *et al.* Natural Variation in Gene Expression Modulates the Severity of Mutant Phenotypes. *Cell* **162**, 391-402 (2015).
57. Lempe, J. *et al.* Diversity of flowering responses in wild Arabidopsis thaliana strains. *PLoS Genet* **1**, 109-18 (2005).
58. Curtis, M.D. & Grossniklaus, U. A gateway cloning vector set for high-throughput functional analysis of genes in planta. *Plant Physiol* **133**, 462-9 (2003).
59. Clough, S.J. & Bent, A.F. Floral dip: a simplified method for Agrobacterium-mediated transformation of Arabidopsis thaliana. *Plant J* **16**, 735-43 (1998).
60. Davis, T.C. *et al.* Arabidopsis thaliana MLO genes are expressed in discrete domains during reproductive development. *Plant Reprod* **30**, 185-195 (2017).
61. Nelson, B.K., Cai, X. & Nebenfuhr, A. A multicolored set of in vivo organelle markers for co-localization studies in Arabidopsis and other plants. *Plant J* **51**, 1126-36 (2007).

62. Jones, D.S. *et al.* MILDEW RESISTANCE LOCUS O Function in Pollen Tube Reception Is Linked to Its Oligomerization and Subcellular Distribution. *Plant Physiol* **175**, 172-185 (2017).
63. Alexander, M.P. Differential staining of aborted and nonaborted pollen. *Stain Technol* **44**, 117-22 (1969).
64. Kumar, S., Stecher, G. & Tamura, K. MEGA7: Molecular Evolutionary Genetics Analysis Version 7.0 for Bigger Datasets. *Mol Biol Evol* **33**, 1870-4 (2016).
65. Felsenstein, J. Confidence-Limits on Phylogenies - an Approach Using the Bootstrap. *Evolution* **39**, 783-791 (1985).

Acknowledgements

We thank Dr. Brian Dilkes, Dr. Daniel S. Jones, Thomas Davis, Yan Ju, and Rachel Flynn for helpful discussions and comments on the manuscript. We thank Dr. Xutong Wang for help with the statistical analysis. Purdue University Start-up funds and a grant from the Oklahoma Center for the Advancement of Science and Technology #PS14-008 to S.A.K. supported this work.

Author contributions

J.Y. and S.A.K. designed the experiments. J.Y. conducted the experiments. J.Y. and S.A.K. analyzed the data and wrote the manuscript.

Competing Interests

The authors declare no competing interests.